Bridging the gap between geometric and algebraic multi-grid methods (extended version)

D. Feuchter[*]   I. Heppner[†]   S.A. Sauter[‡]

G. Wittum[§]

Dedicated to Prof. Dr. W. Hackbusch

Abstract

In this paper, a multi-grid solver for the discretisation of partial differential equations on complicated domains will be developed. The algorithm requires as input only the *given* discretisation instead of a hierarchy of discretisations on coarser grids. Such auxiliary grids and discretisations will be generated in a black-box fashion and will be employed to define purely algebraic intergrid transfer operators. The geometric interpretation of the algorithm allows to use the framework of geometric multigrid methods to prove its convergence.

The focus of this paper is on the formulation of the algorithm and the demonstration of its efficiency by numerical experiments while the analysis is carried out for some model problems.

1 Introduction

In many practical engineering applications, the physical objects under consideration have extremely complicated shape containing a huge number of geometric details on different length scales. In our paper, we shall deal

[*](Dirk.Feuchter@iwr.uni-heidelberg.de), IWR, Universität Heidelberg, Germany

[†](Ingo.Heppner@iwr.uni-heidelberg.de), IWR, Universität Heidelberg, Germany

[‡](stas@amath.unizh.ch), Institut für Mathematik, Universität Zürich, Switzerland

[§](wittum@iwr.uni-heidelberg.de), IWR, Universität Heidelberg, Germany

1

with the numerical solution of elliptic partial differential equations on such domains via the finite element method. Since, practically all, finite element spaces are defined on a finite element partitioning of the physical domain, the complicated shape of the geometry implies that the minimal number of elements in such meshes is necessarily very large. To be more concrete, we focus on applications where the minimal finite element meshes and corresponding (low-order) finite element discretisations of the underlying partial differential equation "nearly" fills the memory of the given computer resources.

In our paper, we will present a simple multi-grid algorithm for the efficient solution of the arising large systems of linear equations. This multi-grid algorithm contains features from both, geometric multi-grid (cf. [18]) and algebraic multilevel methods (cf. [22]). On one hand, the algorithm fits in the framework of geometric multi-grid algorithm being based on (composite) finite element discretisation (cf. [19]) while, on the other hand, the underlying grids may not resolve the geometry and have purely auxiliary character. Our new geometric/algebraic multi-grid algorithm requires as input

- the domain Ω and the corresponding elliptic boundary value problem,

- the algebraic system of linear equations arising from a finite element discretisation,

- the link between geometry and discretisation, i. e., the geometric locations of the degrees of freedom.

The paper is organised as follows. In Section 2, we will introduce an appropriate model problem for the formulation of the multi-grid algorithm which will be presented in Section 3 along with some details on its efficient realisation.

Section 4 is devoted to the convergence analysis of the method. This multi-grid algorithm fits in the framework of geometric multi-grid methods (cf. [18]) and the convergence proof is based on that theory. However, two assumptions which are frequently used in [18] are violated, since,

- the composite finite element spaces are defined on grids which *overlap* the domain but do not necessarily resolve it. The possibly small intersection of a mesh cell with the domain leads to a non-standard scaling in the corresponding stiffness matrix entry and the convergence analysis has to be extended to cover such situations.

2

- The prolongation operators in the multi-grid algorithm are based on interpolation on non-nested grids. As a consequence the proof of the stability of the iterated prolongation is non-trivial.

Section 5 is concerned with numerical experiments. We have performed systematic parameter studies to verify that the convergence of the multi-grid algorithm is by no means restricted to the simplified model problems analysed in Section 4 but carries over to much more general situations. We will apply the multi-grid algorithm to elliptic boundary value problems on practical domains, namely, the Wolfgangsee (Austria) and the "Kieler Förde" (Germany).

The development of multi-grid/-level methods for partial differential equations on complicated domains is a topic of vivid research. Various different approaches exist in the literature as , e.g., *algebraic multi-level methods* (cf. [22], [25], [28], [7], [14], [21], [17], [16]), *coarsening via geometric agglomeration* ([4], [3], [10], [20], [8], [9]), and *coarsening by auxiliary/fictitious space methods* (see [27], [15]). We omit a detailed comparison of the different approaches mentioned above and refer instead to [6]. Due to our knowledge, our approach is the first in the framework of *geometric* multi-grid methods which can be applied conceptually to any given grid and corresponding discretisation. The convergence is analysed in Section 4 for some model problems and we refer to [13] for further details.

2   Model Problem

We will present a multi-grid solver for systems of linear equations arising by discretising elliptic boundary value problems on complicated domains. We restrict to problems with smooth coefficients so that a Poisson-type problem on a complicated domain is an adequate model problem. We assume that the discretisation, i.e., the finite element mesh and the system of equations is given without having a hierarchy of coarse scale discretisations at hand.

Let $\Omega \subset \mathbb{R}^2$ denote a polygonal Lipschitz domain with possibly many geometric details as, e.g., many small holes or complicated boundary. $V := H^1(\Omega)$ denotes the usual Sobolev space while V' is the dual space. Consider the boundary value problem of seeking, for given $F \in V'$, the function $u \in V$ such that

$$a(u, v) = F(v) \qquad \text{for all } v \in V, \tag{1}$$

where the bilinear form $a : V \times V \to \mathbb{R}$ is defined by

$$a\left(u, v\right) := \int_{\Omega} \langle \nabla u, \nabla v \rangle + uv dx. \tag{2}$$

The finite element discretisation is based on a conforming triangulation $\mathcal{G} = \{\tau_1, \tau_2, \ldots \tau_N\}$ in the sense of Ciarlet (cf. [11]). Let S denote the space of continuous, piecewise affine finite elements

$$S := \{u \in V \mid \forall \tau \in \mathcal{G} : u \mid_{\tau} \text{ is affine}\}.$$

The finite element discretisation is given by seeking $u_S \in S$ with

$$a\left(u_S, v\right) = F\left(v\right) \qquad \text{for all } v \in S.$$

The set of vertices of triangles in $\mathcal{G}$ is denoted by Θ and, for $x \in \Theta$, the corresponding local nodal basis by φ_x. The link between a finite element function and its coefficient vector is given via the prolongation

$$P : \mathbb{R}^{\Theta} \to S, \quad P\left[\mathbf{u}\right]\left(x\right) = \sum_{z \in \Theta} \mathbf{u}\left(z\right) \varphi_z\left(x\right).$$

The coefficient vector of the Galerkin solution u_S is the solution of the system of linear equations

$$\mathbf{A}_S \mathbf{u}_S = \mathbf{f}_S \tag{3}$$

with

$$\mathbf{A}_S\left(x, y\right) = a\left(\varphi_y, \varphi_x\right), \qquad \mathbf{f}_S\left(x\right) = F\left(\varphi_x\right) \qquad \text{for all } x, y \in \Theta.$$

Since, for low order discretisations, the linear system (3) typically is very large and sparse, the solution process is a non-trivial task. Multi-grid methods have optimal complexity for solving (3) in the sense that the number of operations only grows linearly with the number of unknowns *provided* a sequence of appropriate coarse scale discretisations is available. However, for problems on complicated domains where only a fine scale discretisation is *given* it is not obvious how to construct a sequence of coarse scale discretisations.

The scope of this paper is to develop a multi-grid algorithm for this type of problem where the convergence behaviour is independent of the number and sizes of the geometric details.

3 Multigrid Algorithm

A multi-grid algorithm is based on a multi-scale discretisation of the boundary value problem. It is a combination of an iterative solver (called smoother) on each discretisation level and a recursive coarse grid correction. Formally, we introduce a parameter $\ell \in \mathbb{N}$ with $0 \leq \ell \leq L$ describing the discretisation level. We start with the *given* fine grid equations (3) and rename them as

$$\mathbf{A}_L \mathbf{u}_L = \mathbf{f}_L,$$

where the number of levels L is not known a-priorily. Analogously, we rename the finite element space S as S_L and its basis as $\varphi_{L,x}$.

3.1 Abstract Multigrid Algorithm

Let $\varphi_{\ell,x}$ denote the standard continuous, piecewise affine Lagrange basis on $\mathcal{G}_\ell$. For any grid function $\mathbf{u} \in \mathbb{R}^{\Theta_\ell}$, we associate a finite element function on the *overlapping domain* Ω_ℓ by

$$P_\ell[\mathbf{u}](x) := \sum_{z \in \mathbb{R}^{\Theta_\ell}} \mathbf{u}(z) \varphi_{\ell,z}(x) \,.$$

From $\Theta_{\ell+1} \subset \overline{\Omega_\ell}$ we conclude that the function $P_\ell[\mathbf{u}]$ can be evaluated at the grid points $\Theta_{\ell+1}$ of the finer mesh. In this light, the inter-grid prolongation $\mathbf{p}_{\ell+1,\ell} : \mathbb{R}^{\Theta_\ell} \to \mathbb{R}^{\Theta_{\ell+1}}$ is defined by

$$\mathbf{p}_{\ell+1,\ell}[\mathbf{u}](x) := P_\ell[\mathbf{u}](x) \,, \qquad x \in \Theta_{\ell+1} \,,$$

and the matrix representation is

$$\mathbf{p}_{\ell+1,\ell} \in \mathbb{R}^{\Theta_{\ell+1} \times \Theta_\ell} : \quad \mathbf{p}_{\ell+1,\ell}(x,y) = P_\ell[\varphi_{\ell,y}](x)$$

for all $x \in \Theta_{\ell+1}$ and $y \in \Theta_\ell$. The restriction is the transposed of $\mathbf{p}_{\ell+1,\ell}$, i.e.,

$$\mathbf{r}_{\ell,\ell+1} \in \mathbb{R}^{\Theta_\ell \times \Theta_{\ell+1}} : \quad \mathbf{r}_{\ell,\ell+1}(x,y) = \mathbf{p}_{\ell+1,\ell}(y,x) \,.$$

Coarse grid operators $\mathbf{A}_\ell$ are recursively defined, for $\ell < L$, via the Galerkin product

$$\mathbf{A}_\ell := \mathbf{r}_{\ell,\ell+1} \mathbf{A}_{\ell+1} \mathbf{p}_{\ell+1,\ell}. \tag{4}$$

In order to define the multi-grid algorithm we have to specify an iterative solver on each single grid. We restrict here to linear solvers of the form

$$\mathbf{u}_\ell^{(i+1)} := \mathbf{u}_\ell^{(i)} - \mathbf{N}_\ell \left(\mathbf{A}_\ell \mathbf{u}_\ell^{(i)} - \mathbf{f}_\ell \right). \tag{5}$$

The application of ν iterations of the form (5) defines a mapping $\mathbf{S}_\ell^{(\nu)} \left(\mathbf{u}_\ell^{(i)}, \mathbf{f}_\ell \right) := \mathbf{u}_\ell^{(i+\nu)}$. The multi-grid algorithm is a recursive procedure which requires as input parameters ν_1, $\nu_2 \in \mathbb{N}$ specifying the number of pre- and postsmoothing steps and a parameter $\gamma \in \{1, 2\}$ controlling whether a V- or a W-cycle is employed (for details we refer to [18]). The multi-grid algorithm is called by

$$\mathbf{u}_L := \mathbf{0}; \qquad \mathbf{mg} \left(\mathbf{u}_L, \mathbf{f}_L, L \right);$$

and defined by

> **procedure mg**$(\mathbf{u}_\ell, \mathbf{f}_\ell, \ell)$;
> **begin**
>   **if** $(\ell = 0)$ **then** $\mathbf{u}_\ell := \mathbf{A}_\ell^{-1} \mathbf{f}_\ell$ **else begin**
> $\mathbf{u}_\ell := \mathbf{S}_\ell^{(\nu_1)} \left(\mathbf{u}_\ell, \mathbf{f}_\ell \right)$;
> $\mathbf{d}_\ell := \mathbf{A}_\ell \mathbf{u}_\ell - \mathbf{f}_\ell$;
> $\mathbf{d}_{\ell-1} := \mathbf{r}_{\ell-1,\ell} \mathbf{d}_\ell$;
> $\mathbf{v}_{\ell-1} := \mathbf{0}$;
>   **for** $j := 1$ **to** γ **do mg**$(\mathbf{v}_{\ell-1}, \mathbf{d}_{\ell-1}, \ell-1)$;
> $\mathbf{u}_\ell := \mathbf{u}_\ell - \mathbf{p}_{\ell,\ell-1} \mathbf{v}_{\ell-1}$;
> $\mathbf{u}_\ell := \mathbf{S}_\ell^{(\nu_2)} \left(\mathbf{u}_\ell, \mathbf{f}_\ell \right)$;
>   **end**;
> **end**;

For the definition of a multi-grid method, the construction of a hierarchy of coarse scale discretisations is the essential step. Once, the systems of linear equations are generated, standard smoothing iterations as, e.g., Gauß-Seidel or variants of ILU-iterations can be applied.

3.2 Generation of a Coarse Grid Hierarchy

In this subsection, we will explain how a hierarchy of coarse scale discretisations can automatically be generated from a given fine grid $\mathcal{G}$ and a corresponding system matrix $\mathbf{A}$. The idea is to assemble a hierarchy of nested

grids $\{\mathcal{G}_\ell\}_{\ell=0}^{L-1}$ which may not resolve the geometric details of the domain while the finest auxiliary grid $\mathcal{G}_{L-1}$ has similar but slightly coarser distribution of mesh cells as $\mathcal{G}$. The auxiliary grids $\mathcal{G}_\ell$ consist mainly of axis-parallel boxes while triangles arise via the green-closure algorithm (cf. [2]). The algorithm starts with a minimal, axis-parallel rectangle (bounding box) satisfying

$$\Omega \subset \tau_0. \tag{6}$$

The coarsest grid is given by $\mathcal{G}_0 = \{\tau_0\}$. Finer triangulations are obtained through an adaptive refinement process which is driven by the distribution of mesh cells in $\mathcal{G}_L$. For a geometric element, e.g., a rectangle, a *regular* subdivision algorithm has to be specified.

Definition 1. *A triangle is refined regularly by connecting the midpoints of edges. A convex quadrilateral is refined regularly by connecting the midpoints of opposite edges.*

Remark 2. *Regular refinement strategies can be defined for three dimensional elements as well.*

The algorithm for assembling the hierarchy of auxiliary grids requires

- the function **control_refine**$(\cdot)$ which controls the adaptation process of the coarse grids to the given grid $\mathcal{G}$. More precisely, an element τ of an auxiliary grid is refined if it contains, at least, $n_{\min}$ elements of the given grid $\mathcal{G}$, where $n_{\min} \in \mathbb{N}$ denotes a control parameter and

$$\textbf{control\_refine}\,(\tau) := \sharp\,\{t \in \mathcal{G} : t \subset \tau\}\,.$$

- For the definition of conforming finite element spaces it might be advantageous to perform a green-closure algorithm after having refined the marked elements to avoid hanging nodes in the grid (cf. [2], [1], [26], [5]) and to enforce refinement of large elements which have small intersection with the domain (cf. Remark 6).

Remark 3. *Numerical experiments indicate that, for finite element meshes on two-dimensional domains, the value $n_{\min} = 4$ is reasonable.*

Remark 4. *If an element $\tau \in \mathcal{G}_\ell$ contains not more than $n_{\min}$ fine grid cells, this is true for all its successors as well.*

7

The algorithm for assembling the auxiliary grid is called by

$$\text{history}\,(\tau_0) := \text{regular}\,; \qquad \textbf{generate\_coarse\_grids}\,(\mathcal{G}_0, 0)$$

and defined by

procedure generate_coarse_grids($\mathcal{G}_\ell, \ell$) ;
begin
    $\mathcal{G}_{\ell+1} := \emptyset$;
    for all $\tau \in \mathcal{G}_\ell$ **do begin**
        if $\text{history}(\tau) = \text{regular}$ **then begin**

        if control_refine $(\tau) \geq n_{\min}$**then begin**   (7)

                refine_regularly(τ) ;
                $\mathcal{G}_{\ell+1} := \mathcal{G}_{\ell+1} \cup sons\,(\tau)$;
                for all $t \in sons\,(\tau)$ **do** $\text{history}(t) := \text{regular}$;
            end else begin
                $\mathcal{G}_{\ell+1} := \mathcal{G}_{\ell+1} \cup \{\tau\}$; $\text{history}(\tau) := \text{irregular}$;
            end;
        end;
    end;
    green_closure($\mathcal{G}_{\ell+1}$) ;
Comment: All elements which are generated during the green-closure
algorithm obtain the attribute $\text{history}(\tau) := \text{irregular}$;

    if $\mathcal{G}_{\ell+1} \neq \mathcal{G}_\ell$ **then generate_coarse_grids**($\mathcal{G}_{\ell+1}, \ell+1$)
    else begin
               $L := \ell+1; \qquad \mathcal{G}_L := \mathcal{G}$;

    end;

Remark 5. *The auxiliary grids are nested in the sense that, for all $\tau \in \mathcal{G}_\ell$ and $\ell < L$, the set of sons is contained in τ*

$$\bigcup_{t \in sons(\tau)} t \subset \tau.$$

The costs for evaluating the function **control_refine** strongly depends on a hierarchical description of the given grid $\mathcal{G}$. The use of an adaptive quadtree leads to an algorithm of linear complexity (up to logarithmic terms).

A quadtree is a tree in which each node either has four descendants (sons) or is a leaf and can be built and used with a complexity of $O(N \log N)$ (cf. [23], [24]). With each node q of the quadtree four values are associated.

1. $box(q)$ is the geometric domain associated with the node q. For the root q_0 of the quadtree, we define $box(q_0) := \tau_0$ (cf. (6)).

2. The set $sons(q)$ is either a set of four tree nodes (set of sons) or the empty set (indicating that q is a leaf).

   The geometric domain $box(q')$ which is linked to some $q' \in sons(q) \neq 0$ is one of the four congruent congruent rectangles arising by refining $box(q)$ regularly (cf. Definition 1).

3. $G(q) \subset \mathcal{G}$ is that subset of the given grid which contains all mesh cells $t \in \mathcal{G}$ with $t \subset box(q)$.

4. $n\_cells(q) := \sharp G(q)$.

We recall the definition of the parameter $n_{\min}$ (cf. (7)) which controls through the function **control_refine** the adaption of the auxiliary grids to the fine grid. This parameter $n_{\min}$ will be used to control the depth of the quadtree as well. Procedure **build_quadtree** is called by

$$box(q_0) := \tau_0; \qquad n\_cells(q_0) := \sharp\mathcal{G}; \qquad \textbf{build\_quadtree}(q_0);$$

with τ_0 as in (6) and defined by

```
procedure build_quadtree(q);
begin
    if n_cells(q) > n_min then
    begin
        generate sons(q) by subdividing box(q) regularly;
        for all q' ∈ sons(q) do begin
            G(q') := {τ ∈ G(q) : τ ⊂ box(q')};
            n_cells(q') := ♯G(q');
            build_quadtree(q');
        end;
    end else sons(q') := ∅;
end;
```

In order to illustrate the work flow of the algorithm we have chosen a given grid $\mathcal{G}$ consisting of 41 triangles and the parameter $n_{\min} := 2$ (cf. Figure 1). The numbering of the sons of a box is counter-clockwise starting with the top right subbox.

This algorithm provides a hierarchical decomposition of the given grid $\mathcal{G}$ based on geometric criteria. For quasi-uniform meshes, it is well known that the complexity of building the quadtree is proportional to $N \log N$. Since the algorithm is driven by the mesh cells of $\mathcal{G}$ it has the flexibility to resolve hierarchically and adaptively the structure of the given mesh $\mathcal{G}$. We have performed numerical experiments for an unstructured given mesh in order to show the efficiency of the quadtree algorithm. The results are depicted in Figure 2 showing clearly that the CPU time behaves proportionally to $N \log N$.

In the next step, the quadtree algorithm will be employed to evaluate the function **control_refine** (τ) (cf. (7)) efficiently. The grid $\mathcal{G}_\ell$ consists of two types of elements:

1. Mesh cells τ which coincide with boxes of nodes in the quadtree (where the number of elements $t \in \mathcal{G}$ with $t \subset \tau$ is already precomputed),

2. further mesh cells which contain not more than $n_{\min}$ elements $t \in \mathcal{G}$.

The attribute history$(\tau) = $ regular indicates that all ancestors of τ have been refined regularly and there exists a unique node in the quadtree $q(\tau)$ with $box(q) = \tau$. Hence, the number of elements of the given grid $\mathcal{G}$ being contained in τ is given by $n\_cells(q)$.

> **function control_refine**(τ) ;
> **begin**
>   determine the node q in the quadtree with $box(q) = \tau$;
>   **control_refine**$(\tau) := n\_cells(q)$;
> **end;**

Remark 6. *Large triangles at the boundary possibly have only small intersection with the domain and might contain not more than $n_{\min}$ triangles. Thus, they are not marked for refinement by the function **control_refine**. Refinement of such triangles is enforced by the green-closure algorithm if neighbouring triangles, e.g., lying in the interior of Ω, are marked for regular refinement.*

Growth of the quadtree | **Triangles of $\mathcal{G}$ which are contained in the quadtree** | **$n\_cells\ (q)$**

given grid $\mathcal{G}$ with $GD(q_{root})$

Initialisation: $box\,(q_0) :=$ bounding box of Ω;
$G\,(q_0) := \mathcal{G}$;
$sons\,(q_0) := \emptyset$.

q_0

compute $n\_cells\,(q_0) := \#\mathcal{G}$

$n\_cells\,(q_0) \geq 2$

refine q_0 regularly

compute $G(q_{1i}),\ 0 \leq i \leq 3$
compute $n\_cells\,(q_{1i}),\ 0 \leq i \leq 3$

q_{10} q_{11} q_{12} q_{13}

$n\_cells\,(q_{10}) < 2$
$n\_cells\,(q_{11}) \geq 2$
$n\_cells\,(q_{12}) \geq 2$
$n\_cells\,(q_{13}) \geq 2$

refine q_{11}, q_{12} and q_{13} regularly

compute $G\,(q_{1ij}),\ 1 \leq i \leq 3,\ 0 \leq j \leq 3$
compute $n\_cells\,(q_{1ij}),\ 1 \leq i \leq 3,\ 0 \leq j \leq 3$

$q_{110} \ldots$ q_{133}

$n\_cells(q_{120}) \geq 2$
$n\_cells(q_{121}) \geq 2$
$n\_cells(q_{1jk}) < 2$
$(j \in \{1,3\},\, 0 \leq k \leq 3)$
$n\_cells(q_{12k}) < 2$
$(k \in \{2,3\})$

refine q_{120} and q_{121} regularly

compute $G(q_{120j}),\ G(q_{121j}),\ 0 \leq j \leq 3$
compute $n\_cells(q_{12ij}),\ (0 \leq i \leq 1,\ 0 \leq j \leq 3)$

$q_{1200} \ldots$ q_{1213}

$n\_cells(q_{1212}) \geq 2$
$n\_cells(q_{120k}) < 2$
$(0 \leq k \leq 3)$
$n\_cells(q_{121k}) < 2$
$(k \in \{0,1,3\})$

refine q_{1212} regularly

compute $G(q_{1212i}),\ 0 \leq i \leq 3$
compute $n\_cells(q_{1212i}),\ 0 \leq i \leq 3$

$q_{12120} \ldots$ q_{12123}

$n\_cells(q_{1212k}) < 2$
$(0 \leq k \leq 3)$

==> END

Figure 1: Work flow of algorithm **build_quadtree** for an example with 41 triangles.
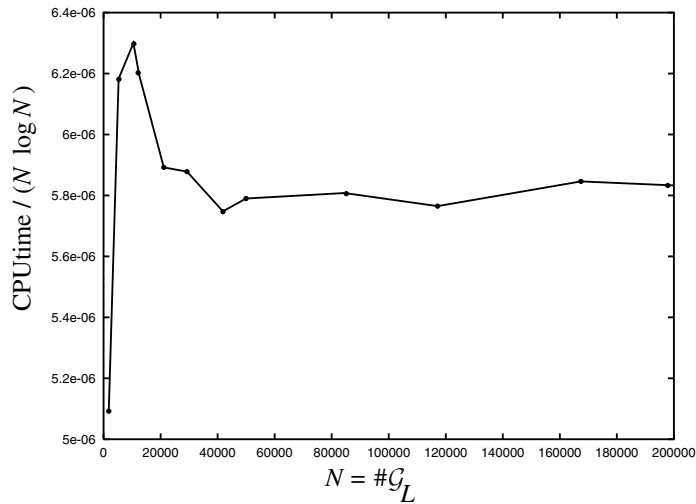
Figure 2: Performance of the quadtree algorithm on an unstructured mesh.

3.3   Prolongation and Restriction

Armed with the hierarchy of coarse grids we proceed to define the prolongation and restriction operators for the multi-grid algorithm. The auxiliary meshes $\mathcal{G}_\ell$ do not resolve the geometry of Ω for $\ell < L$ and, hence, standard finite element spaces on $\mathcal{G}_\ell$ cannot be employed. Instead, we introduce composite finite element spaces based on an iterated prolongation. Let Θ_ℓ denote the set of vertices of triangles in $\mathcal{G}_\ell$ and let $\varphi_{\ell,x}$ be the corresponding (standard) Lagrange basis on $\mathcal{G}_\ell$. The prolongation of a grid function $\mathbf{u} \in \mathbb{R}^{\Theta_\ell}$ is given by

$$P_\ell\left[\mathbf{u}\right](x) = \sum_{z \in \mathbb{R}^{\Theta_\ell}} \mathbf{u}(z)\,\varphi_{\ell,z}(x).\tag{8}$$

The domain covered by the grid $\mathcal{G}_\ell$ is denoted by Ω_ℓ. The definition of the auxiliary grids implies

$$\Omega_{\ell+1} \subset \Omega_\ell \quad\text{and}\quad \Theta_{\ell+1} \subset \overline{\Omega_\ell}.\tag{9}$$

Hence, the function $P_\ell\left[\mathbf{u}\right]$ can be evaluated at the grid points $\Theta_{\ell+1}$ of the finer mesh yielding the intergrid prolongation

$$\mathbf{p}_{\ell+1,\ell}\left[\mathbf{u}\right](x) = P_\ell\left[\mathbf{u}\right](x)\qquad x \in \Theta_{\ell+1}\tag{10}$$

12

with the matrix representation

$$\mathbf{p}_{\ell+1,\ell} \in \mathbb{R}^{\Theta_{\ell+1} \times \Theta_\ell} : \quad \mathbf{p}_{\ell+1,\ell}(x,y) = P_\ell[\varphi_{\ell,y}](x) \quad \text{for all } x \in \Theta_{\ell+1} \text{ and } y \in \Theta_\ell.$$

The restriction is the transposed of $\mathbf{p}_{\ell+1,\ell}$, i.e.,

$$\mathbf{r}_{\ell,\ell+1} \in \mathbb{R}^{\Theta_\ell \times \Theta_{\ell+1}} : \quad \mathbf{r}_{\ell,\ell+1}(x,y) := \mathbf{p}_{\ell+1,\ell}(y,x).$$

By employing the prolongation and restriction operators, all ingredients of the multi-grid algorithm are defined. Some illustrating comments are given below.

Remark 7. *The nestedness of the auxiliary grids (see Remark 5) implies that the composite mapping $\mathbf{p}_{L,\ell} := \mathbf{p}_{L,L-1}\mathbf{p}_{L-1,L-2}\dots\mathbf{p}_{\ell+1,\ell} : \mathbb{R}^{\Theta_\ell} \to \mathbb{R}^{\Theta_L}$ has the representation*

$$\mathbf{p}_{L,\ell}[\mathbf{u}](x) = P_\ell[\mathbf{u}](x) \qquad \forall x \in \Theta_L.$$

Thus, for any coarse grid vector $\mathbf{u} \in \mathbb{R}^{\Theta_\ell}$, the associated composite finite element function has the representation

$$u = P_{L,\ell}[\mathbf{u}] := P_L[\mathbf{p}_{L,\ell}[\mathbf{u}]] = \sum_{z \in \Theta_L} (P_\ell[\mathbf{u}](z)) \varphi_{L,z}. \tag{11}$$

Definition 8. *The space of Composite Finite Elements is the range of $P_{L,\ell}$*

$$S_{L,\ell} := \operatorname{Range} P_{L,\ell} := P_{L,\ell}\left(\mathbb{R}^{\Theta_\ell}\right).$$

The sparsity of the prolongation is concerned in Remark 9.

Remark 9. *Let $x \in \Theta_{\ell+1}$. Then, $\mathbf{p}_{\ell+1,\ell}(x,y) \neq 0$ only for those $y \in \Theta_\ell$ with*

$$x \in \operatorname{int}(\operatorname{supp}\varphi_{\ell,y}),$$

where $\operatorname{int}(M)$ denotes the interior of a set M.

The corresponding weights $\mathbf{p}_{\ell+1,\ell}(x,y)$ can be computed by determining, for each grid point $x \in \Theta_{\ell+1}$, that element $\tau \in \mathcal{G}_\ell$ with $x \in \tau$ and evaluating all shape functions $\{\varphi_{\ell,y}\}_{y:\ vertex\ of\ \tau}$ at x.

The prolongation should be stored in each fine grid point $x \in \Theta_{\ell+1}$ as a list of pairs containing a pointer to the grid point y and the weight $\mathbf{p}_{\ell+1,\ell}(x,y)$ (only if $\mathbf{p}_{\ell+1,\ell}(x,y) \neq \emptyset$).

The definition of the intergrid prolongation has geometric and algebraic character. The construction of the auxiliary grids is based on geometric consideration while these grids are only used for setting up purely algebraic prolongation operators.

4 Convergence Analysis

In this chapter, we will investigate the convergence of the multi-grid method based on non-nested grids following the general multi-grid convergence theory in [18]. However, the proof of the smoothing and approximation property therein differs for discretisations on overlapping and non-nested grids significantly from the situations considered in [18].

The main criteria are

1. The prolongation explained in Section 3.3 is the canonical finite element prolongation on the levels $0...L-1$. Only between the finest auxiliary grid $\mathcal{G}_{L-1}$ and the given grid $\mathcal{G}_L$ the prolongation is non-standard. Hence, concerning the effect of the prolongation on non-nested grids it suffices to consider a *two-grid* method.

2. Since triangles at the boundary, possibly, have only small overlap with the domain, the scaling of the corresponding matrix elements may differ substantially from the nodes lying in the interior of the domain. We will investigate the robustness of the method with respect to these boundary effects.

We recall the basic ingredients of the convergence theory and explain the necessary modifications.

4.1 Smoothing and Approximation Property

In this paper, we will prove the multi-grid convergence in the case that the prolongation is defined on non-nested grids. The effect of the possibly small overlap of large triangles with the domain is studied in detail (for a one-dimension model problem) in [13]. The latter results are summarised here and numerical experiments for the two-dimensional case are reported in Section 5.

4.2 The Effect of the Prolongation on Non-Nested Grids

In this section, we will investigate the effect that the prolongation from the discretisation level $L-1$ to the given discretisation is based on non-nested grids. The effect of triangles having small overlap with the domain is considered in Section 4.3.

Notation 10. *a. For a set G of triangles, the domain covered by the tri-angles is denoted by $\mathrm{dom}\,(G)$, i.e.,*

$$\mathrm{dom}\,(G) := \mathrm{int}\left(\bigcup_{\tau \in G} \overline{\tau}\right).$$

b. For a two-dimensional, open set $M \subset \mathbb{R}^2$, the notation $|M|$ denotes the area measure of M. We use the convention that triangles are open, i.e., $\tau = \mathrm{int}\,(\overline{\tau})$.

c. For mesh-dependent quantities A, B, the notation $A \sim B$ is a shorthand for "There exist constants c and C independent of h_ℓ and ℓ such that $cB \leq A \leq CB$".

For studying the effect of the prolongation on a hierarchy of grids $\{\mathcal{G}_\ell\}_{\ell=0}^{L}$ where $\mathcal{G}_{L-1}$ and $\mathcal{G}_L$ are non-nested we assume that

1. the geometry of Ω is resolved by all grids

$$\Omega = \mathrm{dom}\,(\mathcal{G}_\ell) \qquad \text{for all } 0 \leq \ell \leq L, \tag{12}$$

2. the grids $\{\mathcal{G}_\ell\}_{\ell=0}^{L-1}$ are nested

$$\forall t \in \mathcal{G}_\ell \quad \exists \tau \in \mathcal{G}_{\ell-1} \text{ with } t \subset \tau \qquad \text{for all } 1 \leq \ell \leq L-1,$$

3. the triangulations $\mathcal{G}_\ell$ are quasi-uniform and shape regular.

We start with considering the two grid method. The iteration can be written as an affine map in the form $\mathbf{u}_L^{(i+1)} = \mathbf{K}_L^{TGM}\mathbf{u}_L^{(i)} + \mathbf{R}_L^{TGM}\mathbf{f}_L$ with the two-grid iteration matrix

$$\mathbf{K}_L^{TGM} := \mathbf{K}_L^{\nu_2}\left(\mathbf{A}_L^{-1} - \mathbf{p}_{L,L-1}\mathbf{A}_{L-1}^{-1}\mathbf{r}_{L-1,L}\right)\mathbf{A}_L\mathbf{K}_L^{\nu_1}$$

and the iteration matrix $\mathbf{K}_L := \mathbf{I}_L - \mathbf{N}_L\mathbf{A}_L$ of the linear solver (5). The iteration converges if and only if the spectral radius $\rho\left(\mathbf{K}_L^{TGM}\right)$ is smaller than one. The convergence proof is based on a multiplicative splitting of $\mathbf{K}_L^{TGM}$ and an estimate of the factors in appropriate norms. In this light, we introduce, for $\alpha \in (-1, 1)$, the norm $\|\cdot\|_{\alpha,\ell} : \mathbb{R}^{\Theta_\ell} \to \mathbb{R}$ by

$$\langle \mathbf{u}_\ell, \mathbf{v}_\ell\rangle_{\alpha,\ell} := \left(P_{L,\ell}\,[\mathbf{u}_\ell]\,, P_{L,\ell}\,[\mathbf{v}_\ell]\right)_\alpha,$$

$$\|\cdot\|_{\alpha,\ell} := \langle\cdot,\cdot\rangle_{\alpha,\ell}^{1/2},$$

where $(\cdot, \cdot)_\alpha := (\cdot, \cdot)_{\alpha,\Omega}$ denotes the scalar product in $H^\alpha(\Omega)$ and $\|\cdot\|_\alpha := \|\cdot\|_{\alpha,\Omega} := (\cdot, \cdot)_{\alpha,\Omega}^{1/2}$ the corresponding norm.

Assumption 11. *The two-grid method is applied without post-smoothing, i.e., $\nu_1 = \nu$ and $\nu_2 = 0$.*

The convergence proof for the two-grid method is split into the smoothing property

$$\|\mathbf{A}_L \mathbf{K}_L^\nu\|_{-1+s,\ell\leftarrow 1-s,\ell} \leq C_S \eta(\nu) \tag{13}$$

with $\eta(\nu) \to 0$ as $\nu \to \infty$ and the approximation property

$$\left\|\mathbf{A}_L^{-1} - \mathbf{p}_{L,L-1}\mathbf{A}_{L-1}^{-1}\mathbf{r}_{L-1,L}\right\|_{1-s,\ell\leftarrow -1+s,\ell} \leq C_A$$

for some $s \in (0,1]$. The choice of s is linked to the regularity of the underlying variational problem. Since the purpose of this paper is to develop a multi-grid method on a complicated domain it would be unrealistic to assume full regularity. Let $L : V \to V'$ denote the operator associated with the bilinear form (2).

Assumption 12. *There exists $s \in (0,1]$ such that*

$$L^{-1} : H^{-1+s}(\Omega) \to H^{1+s}(\Omega).$$

To prove the smoothing property (13) we have to assume some technical compatibility conditions relating the given grid $\mathcal{G}_L$ with the auxiliary grid $\mathcal{G}_\ell$. We start with some preparatory Lemmata and introduce first some notations (cf. Figure 3).

For a domain $\omega \subset \mathbb{R}^2$, let T_ω denote a maximal equal-sided triangle in ω and define, for $c > 0$, a scaled version of T_ω (with mass centre M_ω) by

$$T_\omega(c) := \left\{x \in \mathbb{R}^2 \mid \exists \hat{x} \in T_\omega : x = M_\omega + c(\hat{x} - M_\omega)\right\}.$$

Let $D \subset \mathbb{R}^2$ denote a further domain satisfying $\omega \subset D$ and define

$$C_{\omega,D} := \min\left\{c \in \mathbb{R} : D \subset T_\omega(c)\right\} \qquad T_{\omega,D} := T_\omega(C_{\omega,D}). \tag{14}$$

Lemma 13. *Let $\omega \subset D \subset \mathbb{R}^2$ and let $u \in \mathbb{P}_1$ be an affine function. Then,*

$$c\|u\|_{0,D} \leq \|u\|_{0,\omega} \leq \|u\|_{0,D} \tag{15}$$

where c only depends on the constant $C_{\omega,D}$ from (14).

16
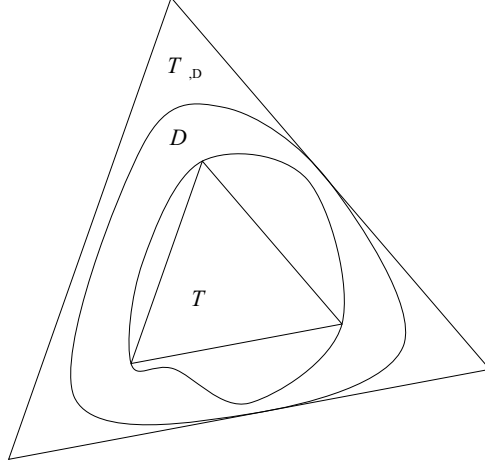
Figure 3: Domain $\omega \subset D$ with largest equal sided triangle $T_\omega \subset \omega$ and smallest scaled triangle $T_{\omega,D}$ containing D.

Proof. The upper estimate is a direct consequence of $\omega \subset D$. For the lower estimate, introduce χ_ω as the affine transformation, mapping the unit triangle $\hat{T}$ (with vertices $(0,0)^\intercal$, $(1,0)^\intercal$, $(0,1)^\intercal$) onto T_ω. Put $c := C_{\omega,D}$. Note that the pullback of $T_{\omega,D}$ (cf. (14)) is the triangle $\hat{T}_c$ with vertices $\frac{1}{3}(1-c,1-c)^\intercal$, $\frac{1}{3}(1+2c,1-c)^\intercal$, $\frac{1}{3}(1-c,1+2c)^\intercal$. The function $\hat{u} := u \circ \chi_\omega$ is affine. Hence:

$$\|u\|_{0,\omega} \geq \|u\|_{0,T_\omega} = \sqrt{\frac{|T_\omega|}{\left|\hat{T}\right|}}\, \|\hat{u}\|_{0,\hat{T}}\,,$$

$$\|u\|_D \leq \|u\|_{0,T_{\omega,D}} = \sqrt{\frac{|T_{\omega,D}|}{\left|\hat{T}_c\right|}}\, \|\hat{u}\|_{0,\hat{T}_c}\,.$$

Since $\mathbb{P}_1$ is finite dimensional and both $\|\cdot\|_{0,\hat{T}}$, $\|\cdot\|_{0,\hat{T}_c}$ are norms on $\mathbb{P}_1$, these norms are equivalent and the constant of equivalence only depends on c. Obviously, $|T_{\omega,D}| / \left|\hat{T}_c\right| = |T_\omega| / \left|\hat{T}\right|$ yielding

$$\|u\|_{0,\omega} \geq C\, \|u\|_{0,D}\,,$$

where C only depends on $C_{\omega,D}$. $\qquad\square$

$\mathcal{G}_l\left(\omega\right)$ $\mathcal{G}_l\left(x\right)$ $\mathcal{G}_l^0\left(\omega\right)$ $\mathcal{N}_l\left(\omega\right)$
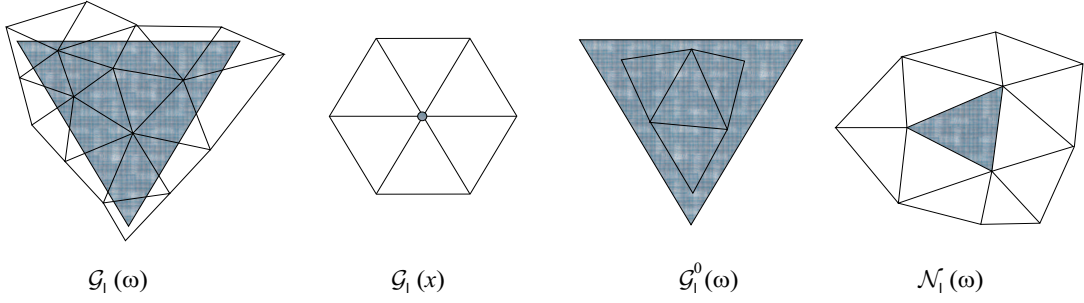
Figure 4: Illustration of the sets $\mathcal{G}_\ell\left(\omega\right)$, $\mathcal{G}_\ell\left(x\right)$, $\mathcal{G}_\ell^0\left(\Omega\right)$, and $\mathcal{N}_\ell\left(\omega\right)$. The domain ω resp. the point x are depicted in blue.

Notation 14. *For $\omega \subset \mathbb{R}^2$ and $x \in \mathbb{R}^2$, we introduce the sets*

$$
\begin{aligned}
\mathcal{G}_\ell\left(\omega\right) &:= \left\{\tau \in \mathcal{G}_\ell : |\tau \cap \omega| > 0\right\}, \\
\mathcal{G}_\ell\left(x\right) &:= \left\{\tau \in \mathcal{G}_\ell : x \in \overline{\tau}\right\}, \\
\mathcal{G}_\ell^0\left(\omega\right) &:= \left\{\tau \in \mathcal{G}_\ell : \tau \subset \omega\right\}, \\
\mathcal{N}_\ell\left(\omega\right) &:= \left\{\tau \in \mathcal{G}_\ell : \overline{\tau} \cap \overline{\omega} \neq \emptyset\right\}.
\end{aligned}
$$

These sets of triangles are illustrated for some examples in Figure 4.

Lemma 15. *Assume that*

$$
\sup_{\tau \in \mathcal{G}_\ell} \frac{|\tau|}{|\mathrm{dom}\left(\mathcal{G}_L^0\left(\tau\right)\right)|} \leq \gamma < \infty. \tag{16}
$$

Then, for the prolongations P_ℓ and $P_{L,\ell}$ (cf. (8) and (11)), the estimate

$$
c_1 \left\|P_\ell \mathbf{u}\right\|_0 \leq \left\|P_{L,\ell} \mathbf{u}\right\|_0 \qquad \forall \mathbf{u} \in \mathbb{R}^{\Theta_\ell} \tag{17}
$$

holds, where c_1 only depends on γ.

Proof. For $\mathbf{u} \in \mathbb{R}^{\Theta_\ell}$, put $u_{L,\ell} := P_{L,\ell}\left[\mathbf{u}\right]$ and $u_\ell := P_\ell\left[\mathbf{u}\right]$. The definition of the prolongation implies that

$$
u_\ell\left(x\right) = u_{L,\ell}\left(x\right) \qquad \text{for all } x \in t \in \mathcal{G}_L^0\left(\tau\right) \text{ and all } \tau \in \mathcal{G}_\ell.
$$

18

Hence, by using Lemma 13

$$\|u_{L,\ell}\|_{0,\Omega}^2 = \sum_{t\in\mathcal{G}_L}\|u_{L,\ell}\|_{0,t}^2 \geq \sum_{\tau\in\mathcal{G}_\ell}\sum_{t\in\mathcal{G}_L^0(\tau)}\|u_{L,\ell}\|_{0,t}^2$$

$$= \sum_{\tau\in\mathcal{G}_\ell}\sum_{t\in\mathcal{G}_L^0(\tau)}\|u_\ell\|_{0,t}^2 \geq C\sum_{\tau\in\mathcal{G}_\ell}\|u_\ell\|_{0,\tau}^2 = C\|u_\ell\|_{0,\Omega}^2$$

where C only depends on γ (cf. (16)). $\qquad\square$

Notation 16. *Two non-identical triangles $\tau_1, \tau_2 \in \mathcal{G}_\ell$ are neighbours if they share a common edge.*

Assumption (16) is relatively restrictive for controlling the refinement process. The refinement might stop relatively early due to the condition that any triangle $\tau \in \mathcal{G}_\ell$ has to contain at least a triangle $t \in \mathcal{G}_L$. If $\mathcal{G}_\ell$ and $\mathcal{G}_L$ have locally comparable step size, Assumption 17 allow further refinement of the auxiliary grids. Before formulating the precise assumption we will explain the underlying idea (cf. Figure 5). Consider a triangle $\tau_1 \in \mathcal{G}_\ell$ such that there exists *no* $t \in \mathcal{G}_L$ with $t \subset \tau_1$. On the other hand, condition (12) implies that there exists a triangle $t_1 \in \mathcal{G}_L$ with non-empty intersection with τ_1. We assume that τ_1 and t_1 have neighbours $\tau_2 \in \mathcal{G}_\ell$ and $t_2 \in \mathcal{G}_L$ satisfying $t_2 \subset \tau_2$ and $\overline{t_1 \cup t_2} \subset \overline{\tau_1 \cup \tau_2}$. If the intersection $t_1 \cap \tau_1$ is not too small we may assume that there exists a vertex P of t_1 with $P \in \tau_1$ and dist $(P, E_{12}) \geq Ch_{\tau_1}$, where E_{12} is the common edge of τ_1 and τ_2. If all these triangles have comparable size we can prove the stability of the intergrid transfer operator.

Assumption 17. *Let all triangles be shape-regular. Assume that, for any $t_1 \in \mathcal{G}_L$, there exists a neighbour $t_2 \in \mathcal{G}_L$ satisfying (cf. Figure 5):*
There exist neighbours $\tau_1, \tau_2 \in \mathcal{G}_\ell$ such that

$$\begin{aligned} t_2 \subset \tau_2, \qquad &\overline{t_1 \cup t_2} \subset \overline{\tau_1 \cup \tau_2}, \\ h_{\tau_1} \sim h_{t_1}, & \\ \text{dist}\,(P, \tau_2) \geq Ch_{\tau_2} \quad &\text{for that vertex } P \text{ of } t_1 \text{ with } P \notin \overline{\tau_2}. \end{aligned} \tag{18}$$

Remark 18. *Assumption 17 along with the shape regularity of the meshes imply (cf. Notation 10 c)*

$$h_{\tau_1} \sim h_{\tau_2} \sim h_{t_1} \sim h_{t_2} \quad \text{and} \quad |\tau_1| \sim |\tau_2| \sim |t_1| \sim |t_2|.$$

Lemma 19. *Under the conditions of Assumption 17 the estimate (17) holds.*

19
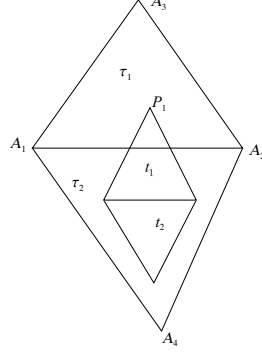
Figure 5: Two coarse grid triangles τ_1, $\tau_2 \in \mathcal{G}_\ell$ covering the fine grid triangles t_1, $t_2 \in \mathcal{G}_L$.

Proof. Adopt the notation of the previous proof and of Assumption 17. We obtain

$$\|u_{L,\ell}\|_{0,\Omega}^2 = \sum_{t \in \mathcal{G}_L} \|u_{L,\ell}\|_{0,t}^2 \geq \frac{1}{4} \sum_{t_1 \in \mathcal{G}_L} \left(\|u_{L,\ell}\|_{0,t_1}^2 + \|u_{L,\ell}\|_{0,t_2}^2 \right)$$

with $t_2 = t_2 (t_1)$ as in Assumption 17. Choose τ_1, τ_2 as in Assumption 17 and denote

the vertices of τ_1 by A_1, A_2, A_3 and those of τ_2 by A_1, A_2, A_4,

the vertex of t_1 contained in τ_1 by P_1 and the others by P_2, P_3.

Then, by using Lemma 15, the shape regularity of the triangles, $h_{\min} := \min \{h_{t_1}, h_{t_2}, h_{\tau_1}, h_{\tau_2}\}$, and the relation $u_{L,\ell} = u_\ell$ on t_2, we obtain

$$\|u_{L,\ell}\|_{0,t_1}^2 + \|u_{L,\ell}\|_{0,t_2}^2 \gtrsim h_{t_1}^2 \sum_{i=1}^{3} u_{L,\ell}^2 (P_i) + h_{\tau_2}^2 \sum_{x:\text{vertex of } \tau_2} u_\ell^2 (x)$$

$$\geq h_{t_1}^2 u_{L,\ell}^2 (P_1) + h_{\tau_2}^2 \sum_{x:\text{vertex of } \tau_2} u_\ell^2 (x)$$

$$= h_{\min}^2 \left\{ \left(\sum_{i=1}^{3} u_\ell (A_i) \varphi_{\ell,A_i} (P_1) \right)^2 + \sum_{x:\text{vertex of } \tau_2} u_\ell^2 (x) \right\}.$$

20

Put $u_i = u_\ell (A_i)$ for $1 \leq i \leq 4$ and $\alpha_i = \varphi_{\ell, A_i} (P_1)$ for $1 \leq i \leq 3$. We obtain

$$\|u_{L,\ell}\|_{0,t_1}^2 + \|u_{L,\ell}\|_{0,t_2}^2 \gtrsim h_{\min}^2 \left\{ \left(\sum_{i=1}^3 u_i \alpha_i \right)^2 + u_1^2 + u_2^2 + u_4^2 \right\}.$$

For $0 < \varepsilon < 1$, we obtain by using $0 \leq \alpha_i \leq 1$:

$$\begin{aligned}
(\alpha_1 u_1 &+ \alpha_2 u_2 + \alpha_3 u_3)^2 + u_1^2 + u_2^2 \\
&= (\alpha_3 u_3)^2 + (\alpha_1 u_1 + \alpha_2 u_2)^2 + 2\alpha_3 u_3 (\alpha_1 u_1 + \alpha_2 u_2) + u_1^2 + u_2^2 \\
&\geq (\alpha_3 u_3)^2 + (\alpha_1 u_1 + \alpha_2 u_2)^2 - (\alpha_3 u_3 \varepsilon)^2 - \left(\frac{\alpha_1 u_1 + \alpha_2 u_2}{\varepsilon} \right)^2 + u_1^2 + u_2^2 \\
&= (\alpha_3 u_3)^2 (1 - \varepsilon^2) + (\alpha_1 u_1 + \alpha_2 u_2)^2 (1 - \varepsilon^{-2}) + u_1^2 + u_2^2 \\
&\geq (\alpha_3 u_3)^2 (1 - \varepsilon^2) + 2 (1 - \varepsilon^{-2}) (u_1^2 + u_2^2) + u_1^2 + u_2^2 \\
&= (\alpha_3 u_3)^2 (1 - \varepsilon^2) + (1 + 2 (1 - \varepsilon^{-2})) (u_1^2 + u_2^2).
\end{aligned}$$

Choosing $\varepsilon = 2\sqrt{2}/3$, we obtain:

$$\|u_{L,\ell}\|_{0,t_1 \cup t_2}^2 \gtrsim h_{\min}^2 \left\{ u_4^2 + \frac{\alpha_3^2}{9} u_3^2 + \frac{3}{4} (u_1^2 + u_2^2) \right\} \gtrsim \|u_\ell\|_{0,\tau_1 \cup \tau_2}^2.$$

The last assumption in (18) implies $\alpha_3 > c$ yielding the proof

$$\|u_{L,\ell}\|_{0,\Omega}^2 \gtrsim \sum_{t \in \mathcal{G}_L} \|u_\ell\|_{0,\tau_1 \cup \tau_2}^2 \gtrsim \|u_\ell\|_{0,\Omega}^2.$$

$\square$

Next, we will establish an estimate of the form $\|P_{L,\ell} \mathbf{u}_\ell\|_0 \leq C_1 \|P_\ell \mathbf{u}_\ell\|_0$. We employ the notations as introduced in Notation 14.

Lemma 20. *Assume that, for all triangles $\tau \in \mathcal{G}_\ell$, there holds $\mathrm{dom}\,(\mathcal{G}_L (\tau)) \subset \mathrm{dom}\,(\mathcal{N}_\ell (\tau))$. Then,*

$$\|P_{L,\ell} \mathbf{u}_\ell\|_0 \leq C_1 \|P_\ell \mathbf{u}_\ell\|_0 \qquad \text{for all } \mathbf{u}_\ell \in \mathbb{R}^{\Theta_\ell}. \tag{19}$$

Proof. Put $u_{L,\ell} = P_{L,\ell} \mathbf{u}_\ell$ and $u_\ell = P_\ell \mathbf{u}_\ell$. By using the assumption of the lemma and the monotonicity of the linear interpolation we obtain

$$\begin{aligned}
\|u_{L,\ell}\|_{0,\mathrm{dom}(\mathcal{G}_L(\tau))}^2 &\leq \max_{x \in \mathrm{dom}(\mathcal{N}_\ell(\tau))} |u_\ell (x)|^2 \sum_{t \in \mathcal{G}_L(\tau)} |t| \\
&\leq \left(\max_{x \in \mathrm{dom}(\mathcal{N}_\ell(\tau))} |u_\ell (x)|^2 \right) |\mathrm{dom}\,(\mathcal{N}_\ell (\tau))|.
\end{aligned}$$

21

Let $t \in \mathcal{N}_\ell(\tau)$ be such that the maximiser in $\max_{x \in \mathrm{dom}(\mathcal{N}_\ell(\tau))} |u_\ell(x)|$ is contained in $\bar{t}$. Then, by using the shape regularity of the meshes we obtain

$$\|u_{L,\ell}\|_{0,\mathrm{dom}(\mathcal{G}_L(\tau))}^2 \leq \frac{|\mathrm{dom}(\mathcal{N}_\ell(\tau))|}{|t|} \left(\max_{x \in \bar{t}} |u_\ell(x)|^2 \right) |t| \leq C \|u_\ell\|_{0,t}^2.$$

Again, by the shape regularity of the mesh we conclude that for any triangle $t \in \mathcal{G}_\ell$ there are only $O(1)$ triangles $\tau \in \mathcal{G}_\ell$ with $t \in \mathcal{N}_\ell(\tau)$ resulting in

$$\|u_{L,\ell}\|_{0,\Omega}^2 = \sum_{\tau \in \mathcal{G}_\ell} \|u_{L,\ell}\|_{0,\tau}^2 \leq \sum_{\tau \in \mathcal{G}_\ell} \|u_{L,\ell}\|_{0,\mathrm{dom}(\mathcal{G}_L(\tau))}^2 \leq C \sum_{t \in \mathcal{G}_\ell} \|u_\ell\|_{0,t}^2 = C \|u_\ell\|_{0,\Omega}^2.$$

$\square$

The next lemma estimates the number of non-zero entries of $\mathbf{A}_\ell$ per row.

Lemma 21. *Assume that, for any $0 \leq \ell \leq L-1$ and any $\tau \in \mathcal{G}_\ell$, there holds*

$$h_t \leq C_2 h_\tau \qquad \text{for all } t \in \mathcal{G}_L \text{ with } \bar{t} \cap \bar{\tau} \neq \emptyset. \tag{20}$$

The number of non-zero entries of $\mathbf{A}_\ell$ is bounded by a constant C_3 depending only on C_2 in (20), the shape regularity and quasi-uniformity of the meshes.

Proof. The matrix entries of $\mathbf{A}_\ell$ have the representation

$$\mathbf{A}_\ell(x,y) = a\left(\varphi_x^{(L,\ell)}, \varphi_y^{(L,\ell)} \right) \tag{21}$$

with $\varphi_x^{(L,\ell)} := P_{L,\ell}\left[\mathbf{e}_x^{(\ell)} \right]$ and the unit grid function $\mathbf{e}_x^{(\ell)} \in \mathbb{R}^{\Theta_\ell}$; $\mathbf{e}_x^{(\ell)}(y) = 1$ for $y = x$ and $\mathbf{e}_x^{(\ell)}(y) = 0$ otherwise. The support of the function $\varphi_x^{(L,\ell)}$ satisfies

$$\mathrm{supp}\, \varphi_x^{(L,\ell)} \subset \bigcup \{ t \in \mathcal{G}_L : |t \cap \mathrm{supp}\, \varphi_{\ell,x}| > 0 \}.$$

The shape regularity of the grids and assumption (20) imply that

$$\mathrm{supp}\, \varphi_x^{(L,\ell)} \subset B_x,$$

where B_x denotes the disc about x with radius $(1+C)\, h_x$ and

$$h_x := \max\{ h_\tau \mid \tau \in \mathcal{G}_\ell(x) \}. \tag{22}$$

The quasi-uniformity of the meshes implies that there exist at most C_3 grid points $y \in \Theta_\ell$ with $B_y \cap B_x \neq \emptyset$, where C_3 only depends on C_2 in (20), the shape regularity and quasi-uniformity of the meshes. The number of non-zero entries of the row $\mathbf{A}(x,\star)$ is bounded by C_3. $\square$

To prove the smoothing property we will need an estimate of the matrix elements $\mathbf{A}_\ell$.

Lemma 22. *Assume (20) and*

$$\sup_{x \in \Theta_\ell} |\mathrm{dom}\,(\mathcal{G}_\ell\,(x))| \geq ch_x^2. \qquad (23)$$

Then,

$$|\mathbf{A}_\ell\,(x,y)| \leq C_4 \quad and \quad \mathbf{A}_\ell\,(y,y) \geq C_5.$$

Proof. In view of (21), the stability estimate of the prolongation operator [19, Theorem 14], and the inverse inequality on shape-regular and quasi-uniform meshes, we obtain

$$|\mathbf{A}_\ell\,(x,y)| = \left|a\left(\varphi_y^{(L,\ell)}, \varphi_x^{(L,\ell)}\right)\right| \leq \left\|\varphi_y^{(L,\ell)}\right\|_{1,\Omega} \left\|\varphi_x^{(L,\ell)}\right\|_{1,\Omega}$$

$$\leq C \left\|\varphi_y^{(L,\ell)}\right\|_{W^{1,\infty}(\Omega)} \left\|\varphi_x^{(L,\ell)}\right\|_{W^{1,\infty}(\Omega)} \sqrt{\left|\mathrm{supp}\,\varphi_y^{(L,\ell)}\right| \left|\mathrm{supp}\,\varphi_x^{(L,\ell)}\right|}$$

$$\leq Ch_\ell^2 \left\|\varphi_{\ell,y}\right\|_{W^{1,\infty}(\Omega)} \left\|\varphi_{\ell,x}\right\|_{W^{1,\infty}(\Omega)} \leq C.$$

For the lower bound, we employ

$$\mathbf{A}_\ell\,(y,y) = a\left(\varphi_y^{(L,\ell)}, \varphi_y^{(L,\ell)}\right) \geq \int_{\mathrm{dom}(\mathcal{G}_\ell(y))} \langle \nabla\varphi_{\ell,y}, \nabla\varphi_{\ell,y} \rangle + \varphi_{\ell,y}\varphi_{\ell,y}dx$$

$$\geq \int_{\mathrm{dom}(\mathcal{G}_\ell(y))} \langle \nabla\varphi_{\ell,y}, \nabla\varphi_{\ell,y} \rangle\,dx.$$

Consider a triangle $\tau \in \mathcal{G}_\ell$ with vertices A, B, C and the shape function $\varphi_{\ell,A}$ on τ corresponding to the node A. Explicit calculations along with the shape regularity and the quasi-uniformity of the mesh show

$$\langle \nabla\varphi_{\ell,A}, \nabla\varphi_{\ell,A} \rangle = \frac{\|B-C\|^2}{4\,|\tau|^2} \gtrsim \gamma h_\ell^{-2}. \qquad (24)$$

Hence,

$$\mathbf{A}_\ell\,(y,y) \geq Ch_\ell^{-2}\,|\mathrm{dom}\,(\mathcal{G}_\ell\,(x))| \geq C.$$

$\square$

Corollary 23. *Let condition (23) be valid. The composite finite element functions satisfy the inverse inequality*

$$\|u\|_1 \leq Ch_\ell^{-1}\,\|u\|_0 \qquad \forall u \in S_{L,\ell}.$$

23

Proof. For the H^1-seminorm $|\cdot|_1 := \|\nabla\cdot\|_0$, we obtain by using (24)

$$|u|_1^2 = \sum_{\tau \in \mathcal{G}_L} \int_\tau \langle \nabla u, \nabla u \rangle \, dz = \sum_{\tau \in \mathcal{G}_L} \sum_{x,y:\text{vertex of } \tau} u(x) \, u(y) \int_\tau \langle \nabla \varphi_x^{(L,\ell)}, \nabla \varphi_y^{(L,\ell)} \rangle \, dz$$

$$\leq \sum_{\tau \in \mathcal{G}_L} \sum_{x,y:\text{vertex of } \tau} u(x) \, u(y) \, h_\ell^{-2} \, |\tau| \leq C \sum_{\tau \in \mathcal{G}_L} \|u\|_{0,\tau}^2 \, h_\ell^{-2} = C h_\ell^{-2} \|u\|_0^2.$$

$\square$

The estimates established in this section compares the matrix entries of $\mathbf{A}_\ell$ with the entries of the system matrix $\mathbf{A}_{\ell,\ell}$ arising by discretising the model problem (2) (with Ω replaced by Ω_ℓ) with standard finite elements on $\mathcal{G}_\ell$. By using these tools the smoothing property for the matrix $\mathbf{A}_\ell$ is analogous to the proof of the smoothing property in the standard case, i.e., for $\mathbf{A}_{\ell,\ell}$. We illustrate this by proving explicitly the smoothing property of the damped Jacobi method

$$\mathbf{u}^{(i+1)} := \mathbf{u}^{(i)} - \omega \mathbf{D}_\ell^{-1} \left(\mathbf{A}_\ell \mathbf{u}_\ell^{(i)} - \mathbf{f}_\ell \right),$$

where $\mathbf{D}_\ell := \operatorname{diag}[\mathbf{A}_\ell]$ and $\omega \in (0,1)$ is the damping parameter.

Theorem 24. *Let the assumptions of Lemma 15, 19, 20, 21, and 22 be fulfilled. The damped Jacobi iteration satisfies the smoothing property (13).*

Proof. For a vector $\mathbf{u}_\ell \in \mathbb{R}^{\Theta_\ell}$, the corresponding composite finite element function is given by (cf. Remark 7)

$$u_\ell := P_{L,\ell}[\mathbf{u}_\ell] := \sum_{y \in \Theta_L} (P_\ell[\mathbf{u}_\ell](y)) \, \varphi_{L,y}(x).$$

For the fine-grid matrix $\mathbf{A}_L$, the smoothing property follows from the quasi-uniformity of the mesh with [18, Proposition 6.2.14].

On coarser grids, we employ

$$\|\mathbf{A}_\ell \mathbf{K}_\ell^\nu\|_{0,\ell \leftarrow 0,\ell} = \left\| \mathbf{A}_\ell \left(\mathbf{I}_\ell - \omega_\ell \mathbf{D}_\ell^{-1} \mathbf{A}_\ell \right)^\nu \right\|_{0,\ell \leftarrow 0,\ell}$$

$$= \omega_\ell^{-1} \left\| \mathbf{D}_\ell^{1/2} \mathbf{X}_\ell \left(\mathbf{I}_\ell - \mathbf{X}_\ell \right)^\nu \mathbf{D}_\ell^{1/2} \right\|_{0,\ell \leftarrow 0,\ell}$$

with $\mathbf{X}_\ell := \omega_\ell \mathbf{D}_\ell^{-1/2} \mathbf{A}_\ell \mathbf{D}_\ell^{-1/2}$.

Below, we will prove that

$$0 \leq \mathbf{X}_\ell \leq \mathbf{I}_\ell \quad \text{and} \quad \left\| \mathbf{D}_\ell^{1/2} \right\|_{0,\ell \leftarrow 0,\ell} \leq C \tag{25}$$

24

holds and, thus, the proof follows from [18, Lemma 6.2.1]. For a grid operator $\mathbf{W}_\ell : \mathbb{R}^{\Theta_\ell} \to \mathbb{R}^{\Theta_\ell}$, the norm $\|\cdot\|_{0,\ell\leftarrow0,\ell}$ is given by

$$\|\mathbf{W}_\ell\|_{0,\ell\leftarrow0,\ell} = \sup_{\mathbf{v}_\ell\in\mathbb{R}^{\Theta_\ell}\setminus\{0\}} \frac{\|P_{L,\ell}\mathbf{W}_\ell\mathbf{v}_\ell\|_0}{\|P_{L,\ell}\mathbf{v}_\ell\|_0}.$$

Lemma 15, 19, and 20 imply

$$c_1\,\|P_\ell\mathbf{v}_\ell\|_0 \leq \|P_{L,\ell}\mathbf{v}_\ell\|_0 \leq C_1\,\|P_\ell\mathbf{v}_\ell\|_0$$

yielding, in combination with the well-known equivalence of the norm $\|P_\ell\cdot\|_0$ with a weighted Euklidean norm, the estimate

$$\|\mathbf{K}_\ell\|_{0,\ell\leftarrow0,\ell} \sim \sup_{\mathbf{v}_\ell\in\mathbb{R}^{\Theta_\ell}\setminus\{0\}} \frac{\|P_\ell\mathbf{K}_\ell\mathbf{v}_\ell\|_0}{\|P_\ell\mathbf{v}_\ell\|_0} \sim \|\mathbf{K}_\ell\|_{\infty\leftarrow\infty} \tag{26}$$

where $\|\cdot\|_{\infty\leftarrow\infty}$ denotes the maximum norm. The number of matrix elements per row of $\mathbf{A}_\ell$ is bounded by C_3 (cf. Lemma 21) and, by combining Lemma 22 with (26), we get
$$\|\mathbf{A}_\ell\|_{0,\ell\leftarrow0,\ell} \leq C.$$
The estimates $\left\|\mathbf{D}_\ell^{-1/2}\right\|_{0,\ell\leftarrow0,\ell} \leq C$ and $\left\|\mathbf{D}_\ell^{1/2}\right\|_{0,\ell\leftarrow0,\ell} \leq C$ are again a consequence of Lemma 22. Altogether, we have proved

$$\|\mathbf{X}_\ell\|_{0,\ell\leftarrow0,\ell} \leq \omega_\ell C$$

and, by choosing $\omega_\ell \leq C^{-1}$ and using the positive definiteness of $\mathbf{X}_\ell$, we established (25). To apply the proofs in [18, Proposition 6.2.14] and [18, 6.3.28] we note that the matrix L_ℓ in [18, Chapter 6.3] is related to the matrix $\mathbf{A}_\ell$ in (4) by
$$L_\ell = \mathbf{M}_{1-s,\ell}^{-1}\mathbf{A}_\ell \tag{27}$$
where the mass matrix $\mathbf{M}_{\alpha,\ell}$ is related to the scalar product $(\cdot,\cdot)_\alpha$ by

$$\mathbf{M}_{\alpha,\ell}\,(x,y) = \left(\varphi_x^{(L,\ell)}, \varphi_y^{(L,\ell)}\right)_\alpha \qquad \text{for all } x,y \in \Theta_\ell.$$

Hence, the proofs in [18, Proposition 6.2.14] and [18, Proposition 6.3.28] imply
$$\|\mathbf{A}_\ell\mathbf{K}_\ell^\nu\|_{-1+s,\ell\leftarrow1-s,\ell} \leq C\eta\,(\nu)$$
with $\eta\,(\nu) \to 0$ as $\nu \to \infty$. $\qquad\qquad\square$

25

For the approximation property, we employ the theory in [18, Chapter 6.3.1.3].

Theorem 25. *Let Assumption 12 and the assumptions of Lemma 15, 19, and 20 be satisfied. Then, the approximation property holds*

Proof. The assumptions of [18, Theorem 6.3.21] are satisfied implying

$$\left\|L_\ell^{-1} - \mathbf{p}_{\ell,\ell-1} L_{\ell-1}^{-1} \mathbf{p}_{\ell,\ell-1}^\star\right\|_{1-s,\ell\leftarrow-1+s,\ell} \leq C_A h_\ell^{2s} \tag{28}$$

where $\mathbf{p}_{\ell,\ell-1}^\star$ is the adjoint of $\mathbf{p}_{\ell,\ell-1}$ with respect to the $\langle\cdot,\cdot\rangle_{1-s,\ell}$- and $\langle\cdot,\cdot\rangle_{1-s,\ell-1}$-scalar product

$$\left\langle\mathbf{p}_{\ell,\ell-1}\mathbf{u}_{\ell-1}, \mathbf{v}_\ell\right\rangle_{1-s,\ell} = \left\langle\mathbf{u}_{\ell-1}, \mathbf{p}_{\ell,\ell-1}^\star\mathbf{v}_\ell\right\rangle_{1-s,\ell-1}.$$

The matrix representation of $\mathbf{p}_{\ell,\ell-1}^\star$ is given by

$$\mathbf{p}_{\ell,\ell-1}^\star = \mathbf{M}_{\alpha,\ell-1}^{-1}\mathbf{p}_{\ell,\ell-1}^\mathsf{T}\mathbf{M}_{\alpha,\ell}$$

with $\alpha = 1 - s$. Replacing L_ℓ in (28) by (27) yields

$$L_\ell^{-1} - \mathbf{p}_{\ell,\ell-1}L_{\ell-1}^{-1}\mathbf{p}_{\ell,\ell-1}^\star = \left(\mathbf{A}_\ell^{-1} - \mathbf{p}_{\ell,\ell-1}\mathbf{A}_{\ell-1}^{-1}\mathbf{p}_{\ell,\ell-1}^\mathsf{T}\right)\mathbf{M}_{\alpha,\ell}.$$

The equivalence of norms (17), (19) and the spectral properties of the mass matrix lead to $\left\|\mathbf{M}_{1-s,\ell}^{-1}\right\|_{-1+s,\ell\leftarrow-1+s,\ell} \leq C h_\ell^{-2s}$ and the approximation property

$$\left\|\mathbf{A}_\ell^{-1} - \mathbf{p}_{\ell,\ell-1}\mathbf{A}_{\ell-1}^{-1}\mathbf{p}_{\ell,\ell-1}^\mathsf{T}\right\|_{1-s,\ell\leftarrow-1+s,\ell} \leq \left\|L_\ell^{-1} - \mathbf{p}_{\ell,\ell-1}L_{\ell-1}^{-1}\mathbf{p}_{\ell,\ell-1}^\star\right\|_{1-s,\ell\leftarrow-1+s,\ell}$$
$$\times \left\|\mathbf{M}_{1-s,\ell}^{-1}\right\|_{-1+s,\ell\leftarrow-1+s,\ell} \leq C_A.$$

$\square$

Since estimate [18, (7.1.2)] holds with $\underline{C}_p = \overline{C}_p = 1$ and [18, (7.1.1)] follows from the Theorem 24, the convergence of the W-cycle is implied by [18, Theorem 7.1.2].

Summarising we have proved that the multi-grid method on non-nested grids converges provided the finest auxiliary grid $\mathcal{G}_{L-1}$ has similar structure as the given grid, i.e., has comparable (slightly coarser) local mesh width.

Although, we do not give a proof for the V-cycle multi-grid method, we will present numerical results for W-cycle and the V-cycle as well.

26
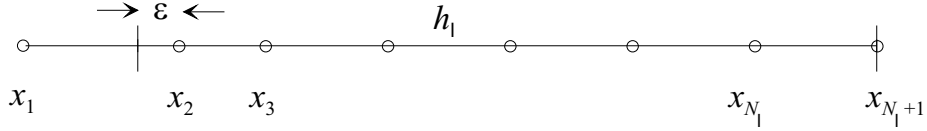
Figure 6: Interval $(0, 1)$ with overlapping grid.

4.3 The Effect of the Small Overlap of Triangles with the Domain Near the Boundary

Since the grid $\mathcal{G}_\ell$ is an overlapping triangulation of the domain, the intersection of triangles at the boundary with the domain might be arbitrarily small. As a consequence the corresponding matrix entries have a very different scaling compared to the interior unknowns. We will study the influence of this scaling effect for a simple model problem.

Let $\Omega = (0, 1)$ and put $V := \{u \in H^1(\Omega) \mid u(1) = 0\}$. Consider the problem of finding $u \in V$ so that

$$a(u, v) = F(v), \qquad \forall v \in H^1(\Omega) \quad \text{with} \quad a(u, v) := \int_\Omega u'v' dx. \qquad (29)$$

To investigate the effect of triangles having small overlap with the domain at the Neumann boundary we consider the following sequence of overlapping grids. For $0 \le \ell \le L$, put $h_\ell = 2^{-\ell}$ and $N_\ell := 2^\ell + 1$. The grid points are given, for $1 \le i \le N_\ell + 1$, by (cf. Figure 6)

$$x_{i,\ell} = \begin{cases} \varepsilon & i = 2, \\ (i - 2) h_\ell & \text{otherwise.} \end{cases}$$

Put $\Theta_\ell^\star := \{x_{i,\ell}\}_{i=1}^{N_\ell+1}$ while, due to Dirichlet's boundary condition at $x = 1$, the unknowns are associated with the set $\Theta_\ell := \{x_{i,\ell}\}_{i=1}^{N_\ell}$. The grid $\mathcal{G}_\ell$ consists of the intervals

$$\tau_{i,\ell} = (x_{i,\ell}, x_{i+1,\ell}), \qquad 1 \le i \le N_\ell.$$

The finite element space S_ℓ is given by

$$S_\ell = \left\{ u \in C^0\left(\overline{\Omega}\right) \mid \forall \tau \in \mathcal{G} : u \mid_\tau \text{ is affine} \right\} \cap V$$

and the finite element discretisation by seeking $u_\ell \in S_\ell$ so that

$$a(u_\ell, v_\ell) = F(v_\ell), \qquad \forall v_\ell \in S_\ell.$$

As a basis of S_ℓ we are choosing the usual nodal basis $\{\varphi_{i,\ell}\}_{i=1}^{N_\ell}$, where the basis functions φ_1, φ_2 are restricted to the domain Ω. Employing the basis representation of u_ℓ and testing with the basis function results in the linear system of equations

$$\mathbf{A}_\ell \mathbf{u}_\ell = \mathbf{F}_\ell$$

with

$$(\mathbf{A}_\ell)_{i,j} := a\left(\varphi_{i,\ell}, \varphi_{j,\ell}\right), \qquad (\mathbf{F}_\ell)_i := F\left(\varphi_{i,\ell}\right).$$

For solving the fine grid equations, a multi-grid method based on the damped Jacobi iteration with damping parameter $1/2$ is employed

$$\mathbf{x}^{(i+1)} = \mathbf{x}^{(i)} - \frac{1}{2}\mathbf{D}_\ell^{-1}\left(\mathbf{A}_\ell \mathbf{x}^{(i)} - \mathbf{b}\right)$$

with iteration matrix $\mathbf{K}_\ell := \mathbf{I} - \frac{1}{2}\mathbf{D}_\ell^{-1}\mathbf{A}_\ell$. As an intergrid transfer operator we employ the canonical finite element prolongation $\mathbf{p}_{\ell,\ell-1} : \mathbb{R}^{\Theta_{\ell-1}} \to \mathbb{R}^{\Theta_\ell}$ and as restriction its transposed. The two grid iteration matrix with ν smoothing steps is given by

$$\mathbf{K}_{\ell,\ell-1}^{TGM} = \left(\mathbf{A}_\ell^{-1} - \mathbf{p}_{\ell,\ell-1}\mathbf{A}_{\ell-1}^{-1}\mathbf{p}_{\ell,\ell-1}^\intercal\right)\left(\mathbf{A}_\ell \mathbf{K}_\ell^\nu\right).$$

The multi-grid convergence will be proved by investigating the smoothing and approximation property in appropriate norms. Although, the model problem has full regularity, i.e., $\|u\|_{2,\Omega} \leq C \|f\|_{0,\Omega}$, the use of the Euklidean norms for the smoothing and approximation property is not appropriate: Numerical experiments show that $\left\|\mathbf{K}_{\ell,\ell-1}^{TGM}\right\|_{0,\ell \leftarrow 0,\ell}$ diverges as $\varepsilon \to 0$ and we have to employ norms with appropriate weights at the Neumann boundary. Put $q_\ell := q_\ell(\varepsilon) := \varepsilon/h_\ell$ and define

$$\mathbf{N}_{s,\ell} := h_\ell \operatorname{diag}\left[q_\ell^{3-s}, 1, 1, \ldots, 1\right].$$

Scalar products and norms on $\mathbb{R}^{\Theta_\ell}$ are defined by

$$\langle \mathbf{u}, \mathbf{v}\rangle_{0,s,\ell} = \mathbf{u}^\intercal \mathbf{N}_{s,\ell}\mathbf{v} \quad \text{and} \quad \|\mathbf{u}\|_{0,s,\ell} := \langle \mathbf{u}, \mathbf{u}\rangle_{0,s,\ell}^{1/2}. \tag{30}$$

The indices $0, s$ indicate that the norm $\|\cdot\|_{0,s,\ell}$ corresponds to a weigthed L^2-norm.

Remark 26. *Straightforward but somewhat technical estimates yield that*

$$c\|P_\ell \mathbf{u}\|_{0,\Omega} \leq \|\mathbf{u}\|_{0,0,\ell} \leq C\|P_\ell \mathbf{u}\|_{0,\Omega}.$$

The proof of the convergence theorem can be found in [13].

Theorem 27. *There exist $0 < \underline{\omega} < \overline{\omega} < 1$, $1 < \underline{\nu} < \overline{\nu}$, and $\overline{q} > 0$ such that*

$$\left\| \mathbf{K}_\ell^{MGM} \right\|_{0,1,\ell \leftarrow 0,1,\ell} \leq 1/2 \qquad \forall\, q \in\,]0,\overline{q}]\,, \quad \nu \in [\underline{\nu},\overline{\nu}]\,, \quad \omega \in [\underline{\omega},\overline{\omega}]\,,$$

where $\mathbf{K}_\ell^{MGM}$ denotes the W-cycle multi-grid iteration matrix with ν steps of the damped Jacobi method as the smoothing iteration.
For $\overline{q} < q < 1$, we have

$$\left\| \mathbf{K}_\ell^{MGM} \right\|_{0 \leftarrow 0} \lesssim (\nu + 1)^{-1}$$

for all $\nu \in \mathbb{N}$.

Summarising we have shown for a one-dimensional model problem that the multi-grid convergence (with respect to a weighted L^2-norm) is robust with respect to a small overlap of elements with the domain. Numerical examples show that this is not the case with respect to the usual L^2-norm: The degree of freedom corresponding to the most left nodal point lying essentially outside of the domain does not converge robustly with respect to the small overlaps. However, this value could be improved (if required) in a post-processing step from the interior nodes via extrapolation.

The model problem under consideration is too simple to draw conclusions to the multidimensional case and complicated boundaries. Further analysis is directed towards the multidimensional case while, in the next chapter, we present numerical results for a two-dimensional model problem.

5   Numerical Experiments

We have performed numerical experiments to verify the efficiency of the proposed multi-grid method. In Step **a**, systematic parameter studies are employed to determine a reasonable value of $n_{\min}$ which controls the refinement of the auxiliary meshes (cf. (7)). These parameter tests include the investigation of the prolongation on non-nested grids and of the effect of possibly small overlaps of triangles with the domain.

In Step **b**, we apply the multi-grid algorithm to elliptic boundary value problems on practical domains, namely, the Wolfgangsee (Austria) and the "Kieler Förde" (Germany).

If not stated otherwise, the test problem is

$$-\Delta u + u = f \quad \text{in } \Omega$$
$$\partial u / \partial n = 0 \quad \text{on } \partial \Omega$$

with $f(x_1, x_2) = x_1$ and the V-cycle multi-grid algorithm is applied with the Gauß-Seidel smoother (one pre- and post-smoothing step).

a1) Nested grids

We have chosen $\Omega = (0,1)^2$ and, as the given grid, a uniform partitioning of Ω into squares. The coarsest auxiliary grid $\mathcal{G}_0$ contains only one element which is Ω. Hence, by choosing $n_{\min} = 4$, the arising multi-grid algorithm is the standard multi-grid method on *nested* grids. Then numerical tests show that the convergence rate decrease with decreasing $n_{\min}$, i.e., with finer auxiliary grids $\mathcal{G}_{L-1}$. However, the CPU-time increases and it turns out that $n_{\min} \in \{4,5\}$ leads to the minimal CPU-times. The following table depicts the dependence of the CPU-time on $n_{\min}$ for a given grid with 65536 degrees of freedom while the results for different grid levels (degrees of freedom) are very similar

$n_{\min}$	3	4	5	6	7
CPU-time in [sec]	206.7	206.5	121.3	118.3	133.4
convergence rate	0.05	0.05	0.06	0.06	0.06

Note that, for $n_{\min} = 4$, the convergence rates are as good as for the standard multi-grid algorithm on nested grids since both versions coincide.

a2) Non-nested grids

Ω and $\mathcal{G}$ are chosen as in the previous example. The coarsest auxiliary grid contains only one element which is the (overlapping) square $(-1/3, 4/3)^2$. In this light, the calculations illustrate the effect of the prolongation on non-nested grids. The numerical tests show that the convergence rates are almost constant for different refinement levels and we choose the grid with 65536 degrees of freedom to illustrate the effect of varying values of $n_{\min}$.

$n_{\min}$	3	4	5	6	7
CPU-time in [sec]	88.7	88.3	85.5	85.7	90.5
convergence rate	0.07	0.07	0.1	0.1	0.2

The tests show that, again, the value $n_{\min} \in \{4,5\}$ is a good choice. While the convergence rates are as small as for test case (**a1**) they are more sensitive with increasing values of $n_{\min}$.

a3) Non-uniform grids

We have checked whether the convergence rates of the multi-grid algorithm are sensitive with respect to possibly non-uniform grid. As a parameter we have chosen the ratio between the largest and the smallest diameter of triangles in the given mesh. We have tested the case $h_{\max}/h_{\min} = 11$. The numerical results show that the convergence rates of our multi-grid-method is independent of this higher ratio. First, we have fixed the degrees of freedom to 108544 and studied the dependence on $n_{\min}$.

$n_{\min}$	3	4	5	6	7
CPU-time in [sec]	168.9	163.4	158.7	153.9	153.5
convergence rate	0.06	0.06	0.09	0.09	0.12

The robust multi-grid convergence rate with respect to the refinement level and the linear dependence of the CPU-time as a function of the number of unknowns are shown in the following table, where we have fixed $n_{\min} = 4$.

level	$\sharp$unknowns	CPU-time in [sec]	$\frac{\text{CPU-time}(\ell)}{\text{CPU-time}(\ell-1)}$	conv. rate
1	106	1.25	−	0.05
2	424	2.09	1.7	0.06
3	1696	5.04	2.4	0.05
4	6784	12.80	2.5	0.05
5	27136	41.89	3.3	0.05
6	108544	163.41	3.9	0.06

a4) Small overlaps

For $\varepsilon > 0$, let $\Omega := (-\varepsilon, 1) \times (0, 1)$. The coarsest auxiliary grid $\mathcal{G}_0$ arises by inserting diagonals (from left bottom to top right) into the squares $(-1, 0) \times (0, 1)$ and $(0, 1) \times (0, 1)$. With decreasing values of ε, the overlap of the two right-most triangles with Ω becomes small. As a test problem we have considered the mixed boundary value problem

$$
\begin{aligned}
-\Delta u &= 1 && \text{on } \Omega, \\
u &= 0 && \text{on } \Gamma_D := \{1\} \times (0, 1), \\
\partial u/\partial n &= 0 && \text{on } \Gamma_N := \partial\Omega \backslash \Gamma_D.
\end{aligned}
$$

The sequence of finite element grids $(\mathcal{G}_\ell)_{\ell=0}^L$ arises by refining $\mathcal{G}_0$ regularly and removing all triangles with empty intersection with Ω. We assume that

31

$\overline{\Omega} = \bigcup_{\tau \in \mathcal{G}_L} \overline{\tau}$ and, hence, the composite finite element space is given by

$$\mathcal{S}_\ell := \left\{ u \in C^0\left(\overline{\Omega}\right) : \forall \tau \in \mathcal{G} : u|_{\tau \cap \Omega} \text{ is affine.} \right\}.$$

We have investigated numerically the dependence of the (non-weighted) Euklidean norm of the two-grid iteration with respect to the parameter $0 < q_\ell := \varepsilon/h_\ell < 1$. As the smoother we have employed the damped Jacobi iteration with two pre- and no post-smoothing steps.

q_ℓ	10^{-1}	10^{-2}	10^{-3}	10^{-4}	10^{-5}
$\ell = 1$	0.43	0.42	0.41	0.41	0.41
$\ell = 2$	0.53	0.53	0.53	0.53	0.53
$\ell = 3$	0.56	0.56	0.56	0.56	0.56
$\ell = 4$	0.56	0.56	0.56	0.56	0.56

The numerical test calculations clearly show that, for the considered range of parameters, the Euklidean norm of the iteration matrix is uniformly bounded away from 1 with decreasing overlap q_ℓ and/or increasing refinement level ℓ.

b) Wolfgangsee, Kieler Förde

In Figure 7, the "Kieler Förde" (Germany) and the "Wolfgangsee" (Austria) are depicted. The given grid is coloured in green while the finest auxiliary grid $\mathcal{G}_{L-1}$ is in black. The adaption to the distribution of mesh cells of the given grid is clearly visible. $\mathcal{G}_{L-1}$ has a similar but slightly coarser triangle distribution as $\mathcal{G}_L$. Note that all elements with empty intersection with Ω will be removed from the meshes. We first have employed the W-cycle and then the V-cycle multi-grid method both with two pre- and two post-smoothing steps of the Gauß-Seidel iteration and fixed the parameter $n_{\min} = 4$.

- V-cycle, Kieler Förde

$\sharp$unknowns	CPU-time in [sec]	$\frac{\text{CPU-time}(\ell)}{\text{CPU-time}(\ell-1)}$	conv. rate	$\sharp$iterations
512	1.5	-	0.188	8
2048	7.6	5.0	0.30	10
8192	42.6	5.6	0.43	13
32768	132.7	3.1	0.47	14
131072	709.5	5.3	0.52	15
524288	3770	5.3	0.68	23
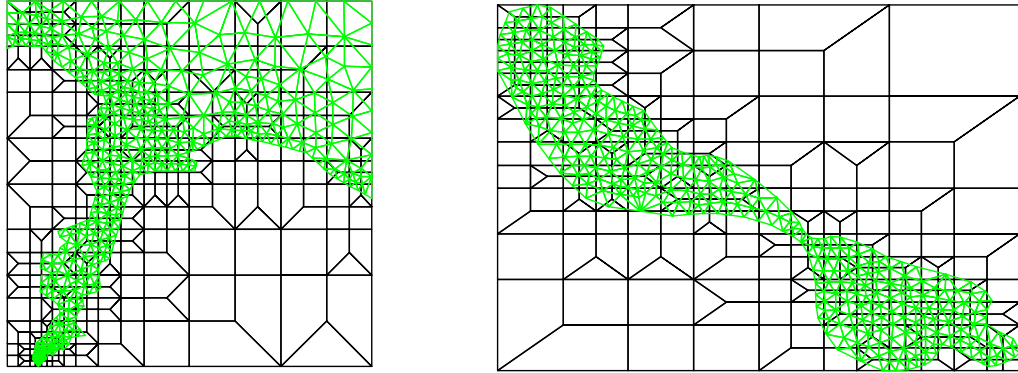
Figure 7: Triangulation of the "Kieler Förde" (left) and the "Wolfgangsee" (right) by the given grid $\mathcal{G}$ (in green) and the finest auxiliary triangulation $\mathcal{G}_{L-1}$.

- V-cycle, Wolfgangsee

♯unknowns	CPU-time in [sec]	$\frac{\text{CPU-time}(\ell)}{\text{CPU-time}(\ell-1)}$	conv. rate	♯iterations
654	0.9	-	2.33e-5	2
2616	3.3	3.5	2.1e-3	3
10464	12.6	3.8	0.01	4
41856	81.1	6.4	0.026	5
167424	344.8	4.2	0.05	6
669696	1791.1	5.2	0.18	10

33

W-cycle, Kieler Förde

♯unknowns	CPU-time in [sec]	$\frac{\text{CPU-time}(\ell)}{\text{CPU-time}(\ell-1)}$	conv. rate	♯iterations
512	2.7	-	0.16	7
2048	22.8	8.4	0.27	9
8192	183.6	8.0	0.33	10
32768	554.8	3.0	0.51	16
131072	3639.3	6.6	0.47	13
524288	19477.3	5.4	0.60	18

- W-cycle, Wolfgangsee

♯unknowns	CPU-time in [sec]	$\frac{\text{CPU-time}(\ell)}{\text{CPU-time}(\ell-1)}$	conv. rate	♯iterations
654	1.3	-	0.00002	2
2616	5.2	4.0	0.002	3
10464	21	4.1	0.01	4
41856	189	8.8	0.03	5
167424	849.9	4.5	0.06	6
669696	5037.1	5.9	0.18	10

We see that the convergence rates, although the geometry of the physical domain is very complicated and the given grid is highly unstructured, are good. The V-cycle multi-grid method performs better than the W-cycle although the convergence rate are slightly larger since the number of operation per cycle is much less compared to the W-cycle. The smallest angles in the given grids are rather small ˜3°. As a consequence, the adaption of the auxiliary grid to the given grid might perform suboptimal leading to the slightly increasing convergence rates. The theoretical investigation in the multi-dimensional case will be presented in [12].

References

[1] R. Bank. *PLTMG user's guide version 6.0*. SIAM, Philadelphia, 1990.

[2] R. Bank and A. Sherman. An adaptive, multi-level method for elliptic boundary value problems. *Computing*, 26:91–105, 1981.

[3] R. Bank and J. Xu. An Algorithm for Coarsening Unstructured Meshes. *Numer. Math.*, 73(1):1–36, 1996.

[4] R. E. Bank and J. Xu. A Hierarchical Basis Multi-Grid Method for Unstructured Grids. In W. Hackbusch and G. Wittum, editors, *Fast Solvers for Flow Problems, Proceedings of the Tenth GAMM-Seminar, Kiel.* Verlag Vieweg, 1995.

[5] P. Bastian. *Parallele Adaptive Mehrgitterverfahren.* Teubner-Verlag, Stuttgart, 1996.

[6] P. Bastian, W. Hackbusch, and G. Wittum. Additive and Multiplicative Multi-Grid - A Comparison. *Computing*, 60:345–364, 1998.

[7] A. Brandt. Algebraic Multigrid Theory: The symmetric case. *Appl. Math. Comput.*, 19:23–56, 1986.

[8] T. Chan, B. Smith, and J. Zou. Overlapping Schwarz methods on unstructured meshes using non-matching coarse grids. *Numer. Math.*, 73:149–167, 1996.

[9] T. Chan, J. Xu, and L. Zikatanov. An agglomeration multigrid method for unstructured grids. *Contemp. Math.*, 218:67–81, 1998.

[10] T. F. Chan and B. F. Smith. Domain Decomposition and Multigrid Algorithms for Elliptic Problems on Unstructured Meshes. *ETNA*, 2:171–182, 1994.

[11] P. Ciarlet. Basic Error Estimates for Elliptic Problems. In P. Ciarlet and J. Lions, editors, *Handbook of Numerical Analysis, Vol. II: Finite Element Methods, (Part 1).* North Holland, Amsterdam, 1991.

[12] N. Frauböse and S. Sauter. Composite Finite Elements and Multigrid. Part II: Convergence Theory in 2-d. *in preparation*.

[13] N. Frauböse and S. Sauter. Composite Finite Elements and Multigrid. Part I: Convergence Theory in 1-d. In W. Hackbusch and U. Langer, editors, *(Electronic) Proceedings of the 17th GAMM-Seminar Leipzig on Construction of Grid Generation Algorithms*, MPI Leipzig, 2001. Preprint no. 11-01, Inst. f. Math, Univ. Zürich, 2001, www.mis.mpg.de/conferences/gamm/2001/GAMM_2001_Proceedings_1.html.

[14] J. Fuhrmann. *Zur Verwendung von Mehrgitterverfahren bei der numerischen Behandlung elliptischer Differentialgleichungen mit variablen Koeffizienten.* PhD thesis, Universität Chemnitz-Zwickau, 1994.

[15] G. Globisch and S. Nepomnyaschikh. The hierarchical preconditioning on unstructured grids. *Computing*, 61:307–330, 1998.

[16] T. Grauschopf, M. Griebel, and H. Regler. Additive multilevel preconditioners based on bilinear interpolation, matrix-dependent geometric coarsening and algebraic multigrid coarsening for second-order elliptic PDEs. *Appl. Numer. Math.*, 23(1):63–95, 1997.

[17] M. Griebel and S. Knapek. A multigrid-homogenization method. In W. Hackbusch and G. Wittum, editors, *Modeling and Computation in Environmental Sciences*, pages 187–202, Braunschweig, 1997. Vieweg. Notes Numer. Fluid Mech. 59.

[18] W. Hackbusch. *Multi-Grid Methods and Applications*. Springer Verlag, Berlin, 1985.

[19] W. Hackbusch and S. Sauter. Composite Finite Elements for the Approximation of PDEs on Domains with Complicated Micro-Structures. *Numer. Math.*, 75(4):447–472, 1997.

[20] B. Koobus, M. Lallemand, and A. Dervieux. Unstructured volume-agglomeration MG: solution of the Poission equation. *Int. J. Numer. Meth. Fluids*, 18, 1994.

[21] J. Mandel, M. Brezina, and P. Vaněk. Energy optimization of algebraic multigrid bases. *Computing*, 62:205–228, 1999.

[22] J. Ruge and K. Stüben. Algebraic multigrid. In S. McCormick, editor, *Multigrid Methods*, pages 73–130, Pennsylvania, 1987. SIAM Philadelphia.

[23] H. Samet. The quadtree and related hierarchical data structures. *Computing Surveys*, 16, 1984.

[24] H. Samet. *The Design and Analysis of Spatial Data Structures*. Addison-Wesley, 1990.

[25] P. Vaněk, J. Mandel, and M. Brezina. Algebraic Multigrid by Smoothed Aggregation for Second and Fourth Order Elliptic Problems. *Computing*, 56(3):179–196, 1996.

[26] R. Verfürth. *A review of a posteriori error estimation and adaptive mesh refinement*. Wiley and Teubner, 1996.

[27] J. Xu. The auxiliary space method and optimal multigrid preconditioning techniques for unstructured grids. *Computing*, 56:215–235, 1996.

[28] P. D. Zeeuw. Matrix-dependent prolongations and restrictions in a black-box multigrid solver. *J. Comp. Appl. Math.*, 33:1–27, 1990.